Low-Pass and High-Pass Filters Consisting of Multilayer Dielectric Stacks

L. YOUNG, SENIOR MEMBER, IEEE, AND E. G. CRISTAL, MEMBER, IEEE

Abstract—Dielectric layers of alternating low and high dielectric constant are useful as filters in the millimeter wave, infrared, and optical regions, spanning a spectrum of about five decades. Transmission line theory can be applied, with refractive index replacing admittance.

The electrical or optical thicknesses of the layers are generally integral multiples of the thinnest layer, but the reflection in the pass band can be appreciably reduced by small adjustments in the layer thicknesses. The theory is based on the concept of Herpin equivalent index, which is the optical counterpart of image admittance used by electrical engineers. The theory is reviewed and design data is presented.

I. Introduction

Dielectric layers or plates can be cascaded to form reflecting filters, both in optics [1]–[4] and at millimeter wave frequencies [5]–[8]. Figure 1(a) shows a quarter-wave stack. It consists of a number of dielectric layers or plates of alternating dielectric constants. The square root of the dielectric constant will be called the refractive index, and will be denoted by the symbol n. Usually, as is indicated in Fig. 1, only two materials are used, and their refractive indices are denoted by n_1 and n_2 in the figure. The electrical or optical thickness of each layer is the same, and is equal to one-quarter wavelength at a particular frequency; at this frequency the maximum reflection is obtained, since all the VSWR's multiply at this frequency to give the input VSWR.

The construction of a multilayer or multiplate dielectric stack, such as is shown in Fig. 1(a), depends on the frequency range. At optical frequencies the layers are usually deposited by evaporation in a vacuum; at microwave frequencies, separate dielectric plates can be assembled. Historically, optical and microwave techniques have developed separately, and so even terminology differs appreciably. In optics, wavelength is taken as the independent variable; in microwaves, frequency is used as the independent variable. In optics, one mostly uses reflectance and transmittance, which represent the reflected and transmitted *powers*, respectively; at microwave frequencies, one mostly expresses the performance as attenuation (in decibels) or VSWR. (We shall use primarily the notation developed by electrical engineers in this paper.)

Figure 2 shows the performance of several quarter-wave stacks as a function of the normalized frequency.

Manuscript received July 9, 1965; revised October 4, 1965. The work reported in this paper was supported by the Rome Air Development Center under Contract AF 30(602)-3174.

The authors are with Stanford Research Institute, Menlo Park, Calif.

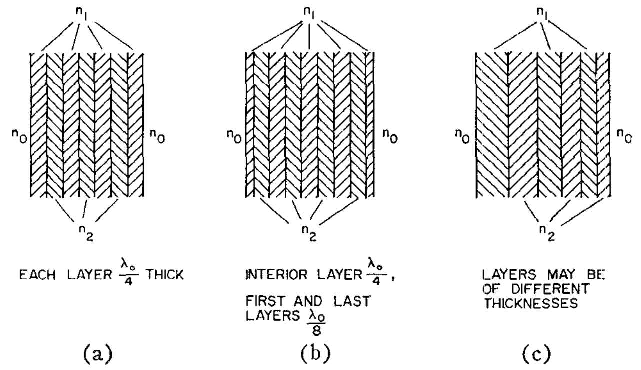

Fig. 1. Three types of dielectric stacks.

(The normalized frequency is defined as the ratio of the actual frequency f to some particular frequency f_0; the particular frequency f_0 in the case of Fig. 2 is that frequency at which each dielectric layer or plate is one-quarter wavelength thick.)

The values of the refractive indices for the curves of Figs. 2 and 3 were chosen because two commonly used optical materials are magnesium fluoride (of refractive index 1.38) and zinc sulfide (of refractive index 2.3), and this makes it easier to compare our computed results with previously published data [3].

The dielectric stacks, the characteristics of which are plotted in Fig. 2, consist of an even number of equal-thickness layers of alternating low and high refractive indices; such a stack is symbolically described by $(LH)^x$, where $2x$ is the total number of layers. The refractive index n_0 of the end media was made equal to the geometric mean of n_1 and n_2, the refractive indices of the layers, for computing the curves in Fig. 2. Thus, n_0 is equal to 1.78. This value of n_0 gives the best match in the middle of the pass bands, which are centered at normalized frequencies of 0, 2, 4, $\cdots$, in Fig. 2, corresponding to layer thicknesses of 0, 180, 360, $\cdots$ electrical degrees. Four cases are shown in Fig. 2; these are two, four, eight, and sixteen layers. As the number of layers is increased, the attenuation rises. At the same time, the ripples in the pass band region also rise; for example, for the case of the sixteen-layer stack, the largest ripple just below the stop band is about $2\frac{1}{2}$ dB high. This is a consequence of the periodic nature of the stack. In order to improve this situation—that is, to reduce the pass-band ripple—one has to resort to some departure from periodicity.

A simple way to improve the match in either the lower or upper pass band, as in Fig. 3, is to use end layers that

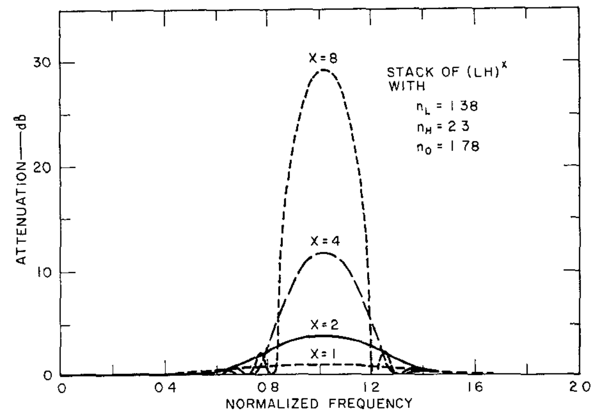

Fig. 2. Attenuation-vs.-frequency characteristics of several stacks of dielectric layers or plates of the same thickness.

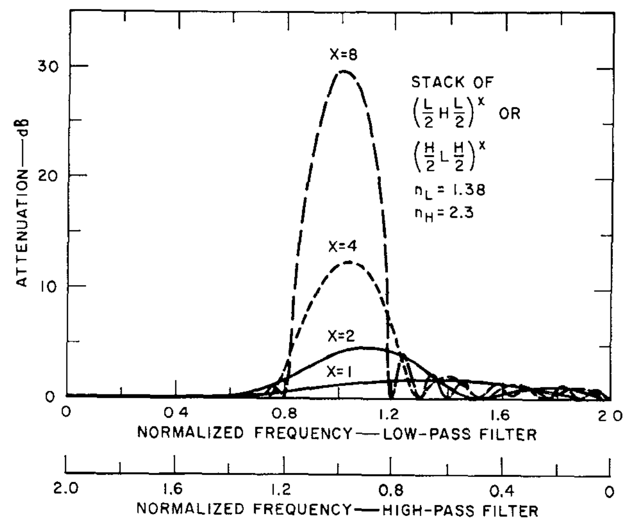

Fig. 3. Attenuation-vs.-frequency characteristics of several stacks of dielectric layers with the two end layers of half the thickness of the interior layers.

are one-half the thickness of the interior layers. Such a stack is represented symbolically by either $[(L/2)H(L/2)]^x$ or $[(H/2)L(H/2)]^x$, where the total number of layers is now $2x+1$, including the two half-thickness end layers.[1] Either type of stack, whether it begins and ends with $L/2$ or with $H/2$, can be used as a low-pass filter, and similarly either type can be used as a high-pass filter. The characteristics are as shown in Fig. 3, where Scale A refers to the low-pass filter and Scale B refers to the high-pass filter. The type of filter that results (low-pass or high-pass) is solely a function of the choice of n_0.

The principal results are summarized here. With either type of filter, a low-pass characteristic results when n_0 is set equal to

$$n_0 = n_1^{1/2} n_2^{1/2}. \tag{1}$$

A high-pass characteristic is obtained where n_0 is set equal to

$$n_0 = n_1^{3/2} n_2^{-1/2}. \tag{2}$$

Let it be emphasized that n_1 refers to the refractive index starting with the exterior layers (see Fig. 1). Thus, for the $[(L/2)H(L/2)]^x$ type of filter, $n_1 = n_L = 1.38$, and $n_2 = n_H = 2.3$, to obtain Fig. 3; whereas for the $[(H/2)L(H/2)]^x$ type of filter, $n_1 = n_H = 2.3$ and $n_2 = n_L = 1.38$. Thus, the numerical solution for n_0 from (2) for the high-pass filter depends on whether the first layer is of lower or higher refractive index. [However, for the low-pass filter, n_1 and n_2 enter (1) symmetrically, and so n_0 is the same for either type, regardless of whether the exterior layers have the lower or higher refractive index.]

The low-pass performance in Fig. 3, Scale A, holds for stacks with n_0 equal to 1.78. Four cases are shown, with $x = 1$, 2, 4, and 8, so that the performance can conveniently be compared with the corresponding curves in Fig. 2. It is seen that the ripples in the lower pass band decrease at the expense of the ripples in the upper pass band.

The high-pass performance in Fig. 3, Scale B, holds both for $[(L/2)H(L/2)]$ stacks with n_0 equal to 1.07 and for $[(H/2)L(H/2)]$ stacks with $n_0 = 2.97$, according to (2). If the refractive index n_0 is different from that required by (1) or (2), as appropriate, then a separate and distinct matching problem exists in matching from a refractive index of $n_1^{1/2} n_2^{1/2}$ or $n_1^{3/2} n_2^{-1/2}$, as the case may be, to a refractive index of n_0; this matching problem can be dealt with by methods described elsewhere, and will not be considered further here. (References are given in [16].)

The performance shown in Figs. 2 and 3 is also fairly representative of the performance to be obtained with stacks of polystyrene plates spaced with layers of air, such as can be used at microwave frequencies. The reason for this is that the ratio of the refractive index of polystyrene to air is 1.6, which is very close to the ratio 2.3/1.38 (which is exactly 5/3).

The pass-band performance in Fig. 3 is better than that in Fig. 2 because the end plates are only half as thick as the interior plates [see Fig. 1(b)]. This can be explained in terms of the concept of image impedance [9], or the Herpin equivalent index [10], [11] which will be explained in Section II.

Further control over the frequency response of a multilayer stack can be exercised by allowing the layers or plates to be of different thicknesses, if necessary. This was first demonstrated by Baumeister [12], [13] and later by some Russian workers [14], [15] using a large electronic digital computer to search for the optimum solution. Image theory, or the Herpin index, can be used at least in some problems to obtain the same or better results with less labor and without the use of a digital computer [16].

The bandwidth of the stop band is determined mostly by the ratio of the two refractive indices of the materials used in the stack, and is independent of the number of

[1] The letters L and H denote layers of low and high index, respectively. The fraction refers to the thickness of the layer. Thus, $L/2$ refers to a layer the electrical or optical thickness of which is half that of a layer denoted by L. (See Fig. 5.).

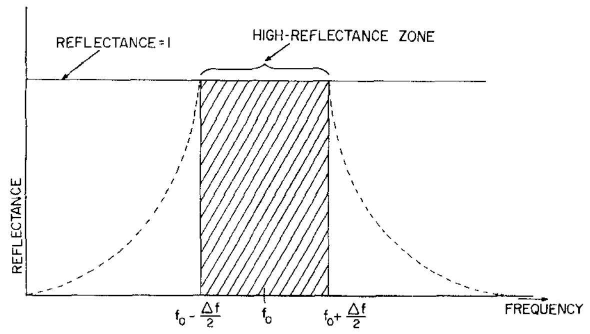

Fig. 4. Typical envelope of a large number of reflectance curves of stacks with different numbers of layers.

plates or layers used. As the number of plates is increased indefinitely, the reflectance-vs.-frequency curve begins to look as shown in Fig. 4. The number of ripples in the pass band increases indefinitely and their peaks form an envelope shown by the broken line in Fig. 4. The high reflectance zone shown shaded in Fig. 4 is centered on a frequency f_0, which is the frequency at which each plate is one-quarter wavelength thick. High reflectance is maintained over a bandwidth Δf centered on the frequency f_0. The characteristics of the curve in Fig. 4 can be worked out from image theory [3], [10], [11]. It can be shown[2] that the fractional bandwidth of the stop band is given by

$$\frac{\Delta f}{f_0} = \frac{4}{\pi}\left[\sin^{-1}\left|\frac{n_1 - n_2}{n_1 + n_2}\right| \text{radians}\right]$$
$$= \frac{1}{45}\left[\sin^{-1}\left|\frac{n_1 - n_2}{n_1 + n_2}\right| \text{degrees}\right]. \qquad (3)$$

For example, if n_1/n_2 is equal to 5/3, then the fractional bandwidth of the stop band given by (3) is close to 32.3 percent, which can also be seen in Figs. 2 and 3.

II. Herpin Equivalent Layer

Any symmetrical combination of dielectric layers can be replaced at any specified frequency by a single dielectric layer having an "equivalent refractive index" and an "equivalent electrical (or optical) thickness" [10], [11], [17]. They are known as the Herpin equivalent index and the Herpin equivalent thickness. (Of course, the equivalent index and equivalent thickness change with frequency.) This concept is basically the same as that of "image admittance" and "image phase constant" [9]. It is further explained in Section IV, where numerical information is also displayed in graphical form.

In summary, dielectric stacks can be built up using symmetrical three-layer stacks such as shown in Fig. 5. It is convenient (but not necessary) to make the thicknesses of the two outer layers equal to exactly one-half the thickness of the central layer. The total electrical thickness of each stack in Fig. 5 is 2θ. There are two cases to be considered. Figure 5(a) shows the first case,

[2] For instance, by setting $A = D = -1$ in (11) of Section IV.

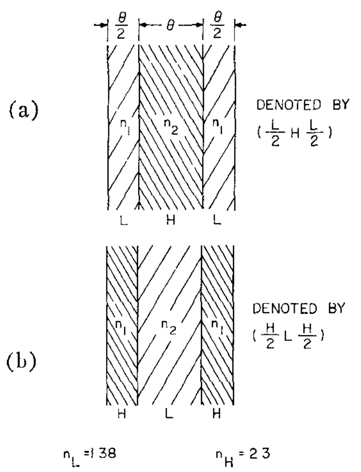

Fig. 5. Basic periods for low-pass and high-pass filters.

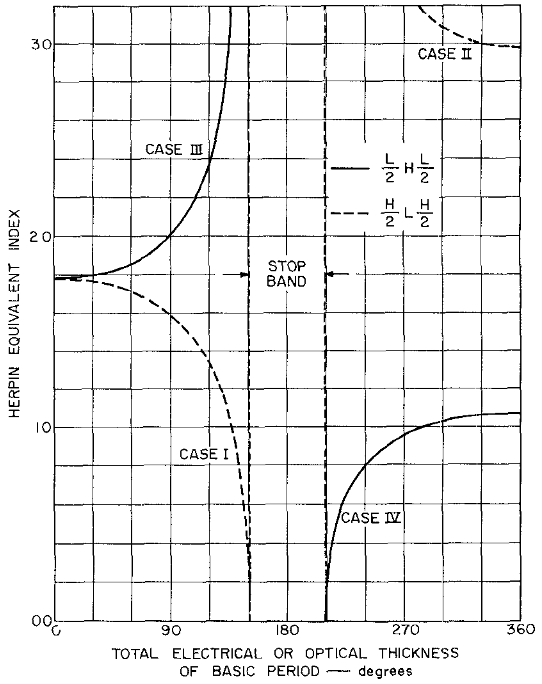

Fig. 6. Herpin equivalent index of the basic period $[(H/2)L(H/2)]$ and of the basic period $[(L/2)H(L/2)]$. (Index of L is 1.38 and index of H is 2.30).

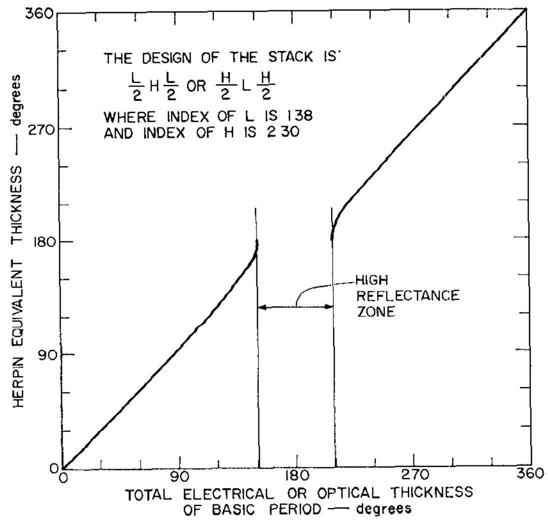

Fig. 7. Herpin equivalent thickness vs. optical thickness.

in which the two outer layers have a refractive index, $n_1 = n_L$, that is less than the refractive index of the central layer $n_2 = n_H$; that is why the two outer layers are marked with an L (for lower), and the central layer is marked with an H (for higher). Figure 5(b) shows the other case, in which the two outer layers have the higher refractive index, $n_1 = n_H$, and are marked with a letter H, while the central layer has the lower refractive index $n_2 = n_L$, and is marked with a letter L.

We shall first illustrate with the special case (common in optics)

$$n_L = 1.38, \tag{4}$$

$$n_H = 2.3. \tag{5}$$

The Herpin equivalent index of the two cases shown in Fig. 5 is plotted as a function of the total electrical or optical thickness 2θ of the basic period in Fig. 6. It is seen that the Herpin equivalent index is not the same in the two cases shown in Fig. 5. The Herpin equivalent thickness is plotted in Fig. 7. In this case the result is the same for both cases shown in Fig. 5. Figures 6 and 7 were obtained by plotting from the equations presented in [11].

III. Transmission Line Equivalence

The transmission ($ABCD$) matrix for a single sheet of dielectric having a relative dielectric constant of ϵ (refractive index $n = \sqrt{\epsilon}$, and a thickness of l, at a wavelength λ, is

$$\begin{bmatrix} \cos\left(\frac{2\pi n l}{\lambda}\right) & j\frac{\eta}{n}\sin\left(\frac{2\pi n}{\lambda}l\right) \\ j\frac{n}{\eta}\sin\left(\frac{2\pi n l}{\lambda}\right) & \cos\left(\frac{2\pi n l}{\lambda}\right) \end{bmatrix} \tag{6}$$

where η is the intrinsic impedance of free space. The $ABCD$ matrix for a transmission line of length l having a characteristic admittance Y_0, at a guide wavelength λ_g, is

$$\begin{bmatrix} \cos\left(\frac{2\pi l}{\lambda_g}\right) & jY_0^{-1}\sin\left(\frac{2\pi l}{\lambda_g}\right) \\ jY_0\sin\left(\frac{2\pi l}{\lambda_g}\right) & \cos\left(\frac{2\pi l}{\lambda_g}\right) \end{bmatrix}. \tag{7}$$

If the identification

$$\lambda_g = \frac{\lambda}{n} \tag{8}$$

and

$$Y_0 = \frac{n}{\eta} \tag{9}$$

is made, the two matrices are identical. Thus, transmission of optical waves through dielectric sheets may be analyzed as transmission of electromagnetic waves along cascaded transmission lines, and vice versa.

IV. Theory

Consider the three cascaded dielectric layers shown in Fig. 5. The layers consist of a dielectric sheet of thickness $\theta/2$ and having a refractive index n_1, followed by a dielectric sheet of thickness θ and having a refractive index n_2, followed by a third layer identical to the first layer. Let the $ABCD$ matrix for the composite be

$$\begin{bmatrix} A & jB \\ jC & D \end{bmatrix}. \tag{10}$$

Epstein [11] and Geppert [9] have shown that[3]

$$A = D = \cos^2\theta - \tfrac{1}{2}(r_{12} + r_{12}^{-1})\sin^2\theta \tag{11}$$

$$B = n_1^{-1}\{\tfrac{1}{2}[1 + \tfrac{1}{2}(r_{12} + r_{12}^{-1})]\sin 2\theta - \tfrac{1}{2}(r_{12} - r_{12}^{-1})\sin\theta\} \tag{12}$$

$$C = n_1\{\tfrac{1}{2}[1 + \tfrac{1}{2}(r_{12} + r_{12}^{-1})]\sin 2\theta + \tfrac{1}{2}(r_{12} - r_{12}^{-1})\sin\theta\} \tag{13}$$

where

$r_{12} = n_2/n_1$

θ = Electrical or optical thickness of the center dielectrical sheet

2θ = Total electrical or optical thickness of the three-layer stack.

The matrix of (10) may also be written as [17]

$$\begin{bmatrix} \cos\gamma & jY_0^{-1}\sin\gamma \\ jY_0\sin\gamma & \cos\gamma \end{bmatrix} \tag{14}$$

where

$$\gamma = \cos^{-1} A \tag{15}$$

and

$$Y_0 = \frac{n_{eq}}{\eta} = \sqrt{\frac{C}{B}} \tag{16}$$

with A, B, C given by (11), (12), and (13), respectively.

As noted by Guillemin [18] and Epstein [11], the cascaded dielectric layers of Fig. 5 are, therefore, equivalent to a single dielectric layer or line having an equivalent refractive index n_{eq} [given by (16)] and an equivalent electrical length of γ radians [given by (15)].

Equation (11) can be used to estimate the stop-band attenuation. In the stop band the cosine term in (14) has an imaginary argument, which is proportional to the attenuation of one Herpin section. The attenuation for x Herpin sections is then

$$\alpha \approx 8.686x \cosh^{-1}\left[\tfrac{1}{2}(r_{12} - r_{12}^{-1})\sin^2\theta - \cos^2\theta\right] \text{ decibels.} \tag{17}$$

This formula is only approximate, and does not take into account the end media. It is, therefore, more accurate when the effect of the end media can be neglected, which is the case when there are a large number of layers in the stack.

[3] The nomenclature used in (11), (12), and (13) differs from the impedance terminology used by Geppert [9]. The correspondence between Geppert's notation and that given here is given by (6) and (7).

Figure 8 gives values of a quantity referred to as the *normalized Herpin equivalent refractive index*, given by (16) with η set equal to unity. Figure 8 is for values of n_L/n_H from 0.1 to 1.0 in steps of 0.1, and for values of θ between 0° and 180°. (Here n_L again represents the lower refractive index, and n_H the higher refractive index.) Two special cases, $n_L/n_H=0.625$ and $n_L/n_H=0.667$, are also given. These latter two cases correspond to ratios of refractive index of air-to-polystyrene and air-to-polyethylene. The quantity n_{eq} is obtained from Fig. 8 as will be explained. There are four cases to consider:

$$\text{Case I, } \left(\frac{H}{2}L\frac{H}{2}\right) \begin{cases} n_2 < n_1; & n_1 = n_H \\ 0 < 2\theta < 180° \end{cases}$$

$$\text{Case II, } \left(\frac{H}{2}L\frac{H}{2}\right) \begin{cases} n_2 < n_1; & n_1 = n_H \\ 180° < 2\theta < 360° \end{cases}$$

$$\text{Case III, } \left(\frac{L}{2}H\frac{L}{2}\right) \begin{cases} n_2 > n_1; & n_1 = n_L \\ 0 < 2\theta < 180° \end{cases}$$

$$\text{Case IV, } \left(\frac{L}{2}H\frac{L}{2}\right) \begin{cases} n_2 > n_1; & n_1 = n_L \\ 180° < 2\theta < 360° \end{cases}.$$

The equivalent index of refraction for all four cases can be obtained from Fig. 8 by the following rules. Define the graph of Fig. 8 as giving the quantity $h=h(2\theta)$. Also, r may now denote either n_2/n_1 or n_1/n_2, whichever is less. Then

1) Case I, $$n_{eq} = n_1 h(2\theta) \tag{18}$$

for $\begin{cases} n_2 < n_1; & n_1 = n_H \\ 0 < \theta < 180° \end{cases}$

2) Case II, $$n_{eq} = \frac{n_1}{h(360° - 2\theta)} \tag{19}$$

for $\begin{cases} n_2 < n_1; & n_1 = n_H \\ 180° < 2\theta < 360° \end{cases}$

3) Case III, $$n_{eq} = \frac{n_1}{h(2\theta)} \tag{20}$$

for $\begin{cases} n_2 > n_1; & n_1 = n_L \\ 0 < 2\theta < 180° \end{cases}$

4) Case IV, $$n_{eq} = n_1 h(360° - 2\theta) \tag{21}$$

for $\begin{cases} n_2 > n_1; & n_1 = n_L \\ 180° < 2\theta < 360° \end{cases}.$

Curves (not normalized) for all four cases are presented in Fig. 6, when the two refractive indices are 1.38 and 2.3, respectively.

The equivalent electrical or optical thickness γ, defined by (15) and denoted as the *Herpin Equivalent Thickness*, is shown in Fig. 9 for Cases I and III (i.e., $0<2\theta<180°$). Define the curves of Fig. 9 as

$$\gamma = \gamma(2\theta). \tag{22}$$

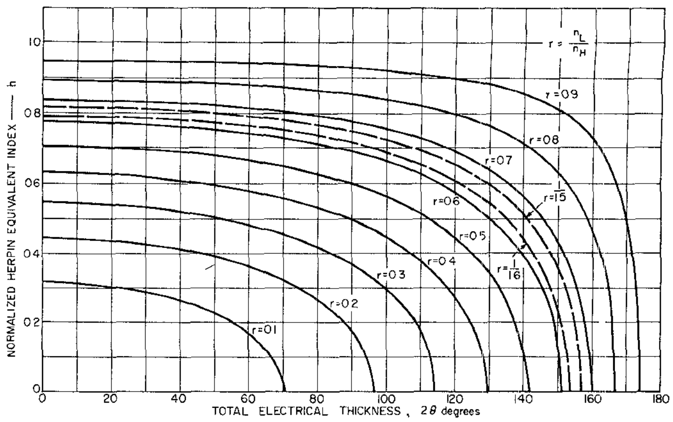

Fig. 8. Graph for determining Herpin equivalent index.

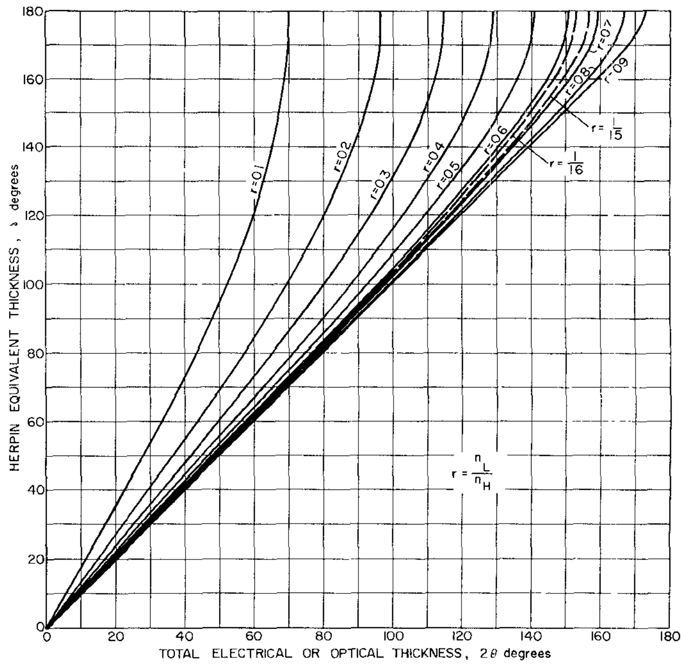

Fig. 9. Graph for determining Herpin equivalent thickness.

Then we have

$$\text{Cases I and III,} \quad \gamma = \gamma(2\theta) \tag{23}$$

for $0 < \theta < 180°$.

$$\text{Cases II and IV,} \quad \gamma(2\theta) = 360° - \gamma(360° - 2\theta) \tag{24}$$

for $180° < 2\theta < 360°$.

V. Reflection Maxima and Minima in the Pass Band

Suppose that the end media are both the same, as for the characteristics in Fig. 3. Then the filter will not reflect whenever its total electrical or optical thickness is a multiple of 180 degrees. Thus, if $x=8$, we look up γ on the ordinate scale at 22.5 degrees, 45 degrees, etc., up to 157.5 degrees, and read 2θ on the abscissa. The lower values of 2θ differ very little from γ, the first value being very close to 22.5 degrees for $r=0.6$. However, the last value is 143 degrees, differing appreciably from 157.5 degrees. Then we can convert to a normalized frequency scale, with $2\theta = 180$ degrees corresponding to a normalized frequency of unity; knowing the symmetry of Fig. 9 (which is as for Fig. 7), we can find all the zero-reflection frequencies in Fig. 3.

The position of the edge of the pass band can also be estimated from Fig. 9. The filter will be matched just outside the stop band, when its electrical or optical total thickness is $(x-1)$ times 180 degrees. Thus, if $x=8$, and $r=0.6$, one looks up the ordinate at $180/x=22.5$ degrees below 180 degrees; then one finds on the abscissa the value 143 degrees, which is 37 degrees below 180 degrees. For a high-pass filter, the pass band would then be expected to extend down to a normalized frequency of $1+37/180=1.21$. This is in fair agreement with Fig. 5 of [16]. At the point where the ordinate scale reaches 180 degrees in Fig. 9, which is also given by (3), the filter already attenuates appreciably.

The positions of the reflection maxima can also be found with the aid of Fig. 9. As before, consider identical end media. Maximum reflection would occur for values of γ equal to an odd multiple of 90 degrees if the Herpin equivalent index were independent of frequency. This criterion enables one to predict all the reflection maxima with very good (but not perfect) accuracy (since the Herpin index does vary with frequency). The values of the reflection maxima are determined from the maximum VSWR, which is very nearly equal to $(n_{eq}/n_0)^{\pm 2}$, whichever sign makes it greater than unity, since the filter is then very nearly an odd number of quarter wavelengths long. The Herpin equivalent index n_{eq} can be determined from Figs. 8 or 6, and n_0 is the refractive index of the end media.

VI. Oblique Angle of Incidence

Dielectric plates or layers can also be used as beam splitters or quasi-optical directional couplers or filters [19], [20]. The same basic theory still applies for that case also. However, the refractive index has to be replaced by a function of the angle of incidence and is different for parallel and normal polarizations.

When the electric vector is normal to the plane of incidence (TE wave), then it can be shown [4] that the *effective refractive index*, n_{eff}, of a medium is

$$n_{eff} = n \cos i, \tag{25}$$

where n is the actual refractive index of the medium, and i is the angle of incidence *inside* the layer.

Similarly, when the electric vector is parallel to the plane of incidence (TM wave), it can be shown [4] that

$$n_{eff} = n/\cos i. \tag{26}$$

When i equals zero (normal incidence), both equations reduce to the statement that the effective refractive index of the medium is equal to n.

The *effective thickness* of each layer for oblique incidence is the actual thickness of the layer multiplied by the cosine of the angle of incidence *inside* that layer. For example, if there were only a single plate of thickness d, its effective thickness is given by $d \cos t$, where t is the angle of transmittance (which is the angle of incidence *inside* the plate, and is given by Snell's law [4]).

VII. Conclusions

The filter properties of dielectric multilayers were discussed. The concept of Herpin equivalent layer makes it possible to simulate refractive index values that may not be physically realizable. Design equations and design curves were presented. They can be used to minimize the pass-band reflection by adjusting the layer thicknesses [16]. The theory is also applicable to beam splitters or directional filters.

References

[1] O. S. Heavens, *Optical Properties of Thin Solid Films*. London: Butterworth, and New York: Academic Press, 1955.
[2] A. Vašiček, *Optics of Thin Films*. Amsterdam: North-Holland Publishing Company, and New York: Interscience Publishers, 1960.
[3] P. W. Baumeister, *Handbook of Optical Design*, MIL-Handbook No. 141, 1962, October 5, ch. 20, obtainable from Control Center 550, Frankford Arsenal.
[4] M. Born and E. Wolf, *Principles of Optics*. New York: Pergamon Press, 1964, Section 1.6.
[5] A. F. Harvey, *Microwave Engineering*. New York: Academic Press, 1963.
[6] A. F. Harvey, "Optical techniques at microwave frequencies," *Proc. I.E.E.*, Part B, vol. 106, pp. 141–157, March 1959.
[7] L. Young and P. W. Baumeister, "Microwave and optical interference filters—some similarities and differences," *NEREM Record*, vol. 5, pp. 8–9, 1963.
[8] W. Culshaw, "Reflectors for a microwave Fabry-Perot interferometer," *IRE Trans. on Microwave Theory and Techniques*, vol. *MTT-7*, pp. 221–228, April 1959.
[9] D. V. Geppert, "Image-impedance design of TEM mode microwave filters," Sylvania Electronic Defense Laboratory, P.O. Box 205, Mountain View, Calif., November 1, 1955.
[10] A. Herpin, "Optique Électromagnétique," *Comptes Rendus*, vol. 225, pp. 182–183, 1947.
[11] L. I. Epstein, "The design of optical filters," *J. Opt. Soc. Am.*, vol. 42, pp. 806–810, November 1952.
[12] P. W. Baumeister, "Design of multi-layer filters by successive approximations," *J. Opt. Soc. Am.* vol. 48, pp. 955–958, December 1958.
[13] P. W. Baumeister and J. M. Stone, "Broad-band multilayer film for Fabry-Perot interferometers," *J. Opt. Soc. Am.*, vol. 46, pp. 228–229, March 1956.
[14] A. M. Ermolaev, I. M. Minkov, and A. G. Vlasov, "Method for the calculation of a multilayer coating with a given reflectivity," *Optika I Spektroskopiya*, vol. 13, English Translation, pp. 142–146, August 1962.
[15] R. S. Sokolova and T. N. Krylova, "Multilayer dielectric systems with films of unequal optical thickness," *Optika I Spektroskopiya*, vol. 12, English Translation, pp. 437–440, June 1962.
[16] L. Young and E. G. Cristal, "On a dielectric multilayer filter by Baumeister," *Appl. Optics*, to be published, January 1966.
[17] P. H. Berning, "Use of equivalent films in the design of infrared multilayer antireflection coatings," *J. Opt. Soc. Am.*, vol. 52, pp. 431–436, April 1962.
[18] E. A. Guillemin, *Communication Networks*, New York: 1935, pp. 161–184.
[19] J. J. Taub, H. J. Hindin, and G. P. Kurpis, "Quasi-optical waveguide filters," *IEEE Trans. on Microwave Theory and Techniques* (*Correspondence*), vol. MTT-12, pp. 618–619, November 1964.
[20] R. Levy, "Directional couplers," in *Advances in Microwaves*, vol. I, L. Young, Ed., New York: Academic, to be published.
[21] C. Dufour and A. Herpin, "Propagation des ondes électromagnétiques dans un milieu stratifié périodique transparent," *Revue d'Optique*, vol. 32, pp. 321–348, June 1953.